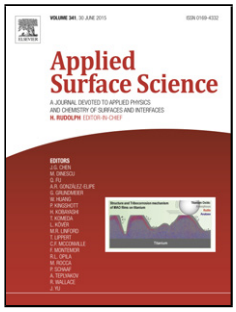

Title: Electrosorption of a modified electrode in the vicinity of phase transition: A Monte Carlo study

Authors: E.M.Gavilán Arriazu, O.A. Pinto

PII: S0169-4332(17)32974-4
DOI: https://doi.org/10.1016/j.apsusc.2017.10.051
Reference: APSUSC 37394

To appear in: *APSUSC*

Received date: 5-7-2017
Revised date: 25-9-2017
Accepted date: 7-10-2017

Please cite this article as: E.M.Gavilán Arriazu, O.A.Pinto, Electrosorption of a modified electrode in the vicinity of phase transition: A Monte Carlo study, Applied Surface Science https://doi.org/10.1016/j.apsusc.2017.10.051

Electrosorption of a modified electrode in the vicinity of phase transition: A Monte Carlo study

E.M. Gavilán Arriazu and O. A. Pinto*

[1]*Instituto de Bionanotecnología del NOA (INBIONATEC-CONICET), Universidad Nacional de Santiago de Estero, RN 9 Km 1125 Villa el Zanjón, Santiago del Estero, G4206XCP, Argentina*

* Corresponding author: oapinto@unsl.edu.ar

Graphical abstract

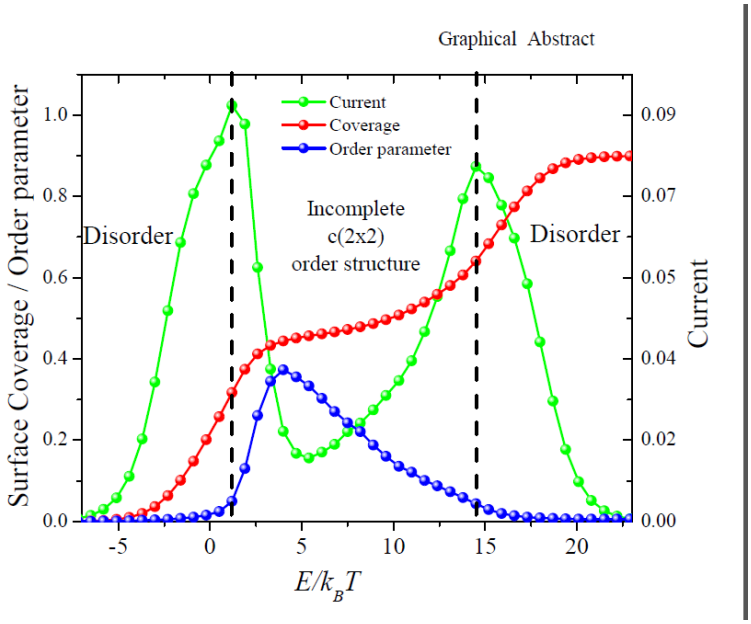

Highlights:

- Monte Carlo simulation was used to study the electrosorption of a electroactive specie on the surface of a modified electrode.
- This model is able to reproduce the main physico-chemical behavior of a on electroactive specie on a modified electrode surface in the presence of a non electroactive species.
- The analysis was based on the study of voltammograms, order parameters, isotherms, configurational entropy per site, in several possible scenarios at different energies and degrees of coverage of non-electroactive species.

Abstract

We present a Monte Carlo study for the electrosorption of an electroactive species on a modified electrode. The surface of the electrode is modified by the irreversible adsorption of a non-electroactive species which is able to block a percentage of the adsorption sites. This generates an electrode with variable connectivity sites. A second species, electroactive in this case, is adsorbed in surface vacancies and can interact repulsively with itself. In particular, we are interested in the analysis of the effect of the non-electroactive species near of critical regime, where the c(2x2) structure is formed. Lattice-gas models and Monte Carlo simulations in the Gran Canonical Ensemble are used. The analysis conducted is based on the study of voltammograms, order parameters, isotherms, configurational entropy per site, at several values of energies and coverage degrees of the non-electroactive species.

Keyword: Monte Carlo simulation; lattice-gas model; modified electrode surface; voltammograms, electrosorption.

1. Introduction

In the last years, computational models have been an important tool to understand physicochemical process that occurs in interfaces. The possibility of manipulate parameters gives to the modeling and simulation methods an added value to study and understand complex systems that cannot be approached in a practical way. With these tools, electrochemical processes has been studied applying various methodologies, such as: mathematical equations and stochastic and digital simulations, just to name a few [1–6] However, some aspects of the problem remain unexplored, like critical behavior and charge transfer at modified electrodes.

Standard Monte Carlo (MC) simulation [7–9] is one of the most commonly used strategies to understand phenomena occurring on surfaces [10, 11] and study electrochemical processes [12, 13]. The electrode surface is easily mimicked by a lattice-gas model where each site of the lattice is a position of the crystalline structure of the substrate where an electroactive species can be adsorbed [14]. For example, with these techniques, the adsorption of bromide on Ag(100) has been studied and contrasted with experimental data, given very acceptable results [15–18].

When an electroactive species, with lateral interactions, is adsorbed on the electrode surface, several interesting phenomena occur. For example, it was observed experimentally the formation of critical clusters of ordered 2-D adsorbed layers in the underpotential region in Ag(hkl) on Pb^{2+} [19]. Other phenomenon observed was the deposition of bromide on an Ag(001) electrode which shows a second order phase transition and form a c(2x2) ordered structure. This was investigated using in situ x-ray scattering methods [20]. The c(2x2) ordered structure was observed in other experimental systems [21]. In [22] the authors relate, in the critical regime, the inflexion point of the isotherms with the current peak of voltammograms for lead deposition on silver single crystal surfaces, this link the surface coverage with the charge transference to the electrode.

The modification of electrode surfaces is an easy way to emulate amorphous solids, where the connectivity of each adsorption site varies. Thus, the electrosorption phenomenon in modified surfaces is equivalent to the adsorption on heterogeneous solid surfaces [23–25] In References [26] and [27] heterogeneity was introduced by random dilution of bonds between the particles adsorbed at nearest-neighbor sites in a triangular lattice, with repulsive interactions. The authors claim that the order is destroyed at very low bond dilutions and the critical temperatures of the transitions decrease with the degree of disorder.

Furthermore, the modification of the substrate has practical applications. In electrocatalysis and heterogeneous catalysis occurring at surfaces, is well known the influence of the SBE's (site blocking elements) in the catalytic process, acting as an element who turn off the active sites and could accelerate or decelerate the reaction rate [28–30]. In reference [31] the SBE has been applied as an indirect method to understand the type of oxygen interaction with a Pt(111) electrode surface. Following the catalytic phenomena, Leiva [32] proposed a model to explain how the nature and the surface coverage of adatoms affect the catalytic activity. Metal substitution (point defects) in spinel cathodes for lithium-ion batteries stabilize the structure, improving the cycle life [33]. The influence of this point defects in a spinel cathode was addressed with MC simulations [34].

There are several electrochemical techniques applied to obtain surfaces data, this is crucial to understand the state of a modified electrode. Voltammetry is maybe the more used of all them, in special cyclic and linear potential programs [35, 36]. In a previous work, an electrode surface has been modified by the irreversible deposition of an artificial clay (Laponite®), while a redox probe $Fe(CN)_6^{4-}$ was responsible of the charge transference; this system was studied by experimental and computer simulated voltammograms [37].

The main aims of the present work are (i) to identify and characterize the effect of defects on the electrodeposition process in the neighborhood of the critical regime of the c(2x2) order structure; (ii) to draw general conclusions on the effect of the impurities on the linear sweep rate voltametric curves; and (iii) to provide the basis for the evaluation of experimental findings in modified electrodes.

The paper is organized as follows: In Section 2, the lattice-gas model and details of Monte Carlo simulations are presented. Results and discussion are presented in Section 3. Finally, the conclusions are drawn in Section 4.

2- **Monte Carlo simulation and basic definitions**

The electrosorption process can be modeled considering an electrode surface as a square lattice with $M=L^2$ adsorption sites predefined, being L the lateral size. The charge transference mechanism is as follow: when an electroactive species, called *A*, is deposited at the surface, an electron is transferred from interphase to the electrode bulk. In reverse, when an electroactive particle is desorbed from the electrode an electron is expulsed. However, two electrons cannot be transferred in the same direction consecutively. This can be expressed by the next equation for a charged particle A^-

$$A^- + * \leftrightarrow A_{ads} + e^- \qquad (1)$$

where (*) denote an empty site, A_{ads} the *A*-species adsorbed and e^- is the elementary charge unit.

The electrode surface can be modified by the irreversible deposition of a non-electroactive species in the range of the work potential, called *B*. The main role of this species is blocking the charge transfer sites. If N_B sites are blocked in the substrate, then M - N_B are the available sites for deposition of *A*-species. The surface density of blocked sites is monitored by $\sigma = N_B / M$, if $\sigma = 0[1]$ the substrate is empty[full].

Both species cannot interact with each other. Only interactions, *w*, between *A* particles are considered. The Hamiltonian can be expressed by:

$$H = \frac{1}{2} w \sum_{<i,j>} c_i c_j - \mu \sum_{i}^{M} c_i \qquad (2)$$

where c_i is the occupation variable of the *i*-th site, which takes the value 1 if the site is occupied by *A* and 0 in any other case. Here μ is the chemical potential. The first and second sum runs over all nearest-neighbors (NNs) pairs and all available sites respectively. In this

work, repulsive interactions (w>0) are considered. This is essential to consider the formation of the order structure called c(2x2).

The chemical potential associated to the deposition process can be connected to the electrochemical potential (E) with the dilute-solution approximation as [12].

$$\mu = \mu_0 + k_B T \ln\left(\frac{C}{C_o}\right) - \gamma e^{-} E \tag{3}$$

where μ_0 is a chemical reference potential, $k_B T$ is temperature expressed as relative units of the Boltzmann constant, k_B. C and C_0 are bulk ionic concentration and a reference concentration, respectively. γ is the electrosorption valence [38, 39], γe^{-} is the charge transferred through the external circuit. This study assume that γ is constant [40, 41].

The current I in the voltammograms, can be obtained in the grand canonical assembly via the normalized mean square fluctuations [42–44] of the adsorbed phase. Without loss of generality, the dimensionless current (i) can be expressed [14, 37 , 45, 46] as:

$$i = \frac{I}{\gamma e^{-} \nu \Gamma} = \frac{1}{M}\frac{\partial \langle N_A \rangle}{\partial E} = \frac{\langle N_A^2 \rangle - \langle N_A \rangle^2}{M} \tag{4}$$

here Γ , is the number of adsorption sites per unit surface area, ν is the sweep rate and $< N_A >$, are average of the particles deposited. Is important to observe that $\theta = < N_A >/M$ is the average coverage of the species A on surface. In this work a linear sweep of potential is considered.

To monitor the low-temperature ordered phase c(2x2), is useful to define an order parameter as [47] ,

$$\Psi \equiv \frac{|\theta_1 - \theta_2|}{2} \qquad (5)$$

where θ_1 and θ_2 are the average coverage of two sub-lattices, 1 and 2 respectively, trivially defined in the ordered structure, as is shown in figure 1. This definition considers the two possible configurations (or degenerations) of the structure. When $\Psi = 1$, the pure structure is formed, thus, complete order can be identified. But, when $\Psi = 0$, the particles are in a disordered configuration over the substrate.

Other magnitude, useful to describe the order, is the configurational entropy per site, defined by fluctuations theory as:

$$\frac{ds}{d\theta} \equiv \frac{1}{T}\left[q_d - \mu\right] = \frac{1}{T}\left[\frac{\langle HN_A\rangle - \langle H\rangle\langle N_A\rangle}{\langle N_A^2\rangle - \langle N_A\rangle^2} - \mu\right] \qquad [6]$$

where $q_d = \langle HN_A\rangle - \langle H\rangle\langle N_A\rangle / \langle N_A^2\rangle - \langle N_A\rangle^2$ is the differential heat associated to the deposition process [10]. From equation (6), the integral entropy can be obtained by:

$$S \equiv \int_{\theta=0}^{\theta=1} s(\theta) d\theta \qquad [7]$$

The adsorption-desorption equilibrium process is simulated by Monte Carlo technique in the Grand Canonical Ensemble, using the Glauber algorithm[4, 48]. The Metropolis scheme [49] is used to satisfy the principle of detailed balance.

Initially, the empty lattice is filled randomly with a density σ. The species *A* will adsorb or desorb. Thus, it is considered the modified surface in contact with a particle *A* reservoir, at a temperature T and potential *E*. A Monte Carlo step (MCS) is achieved when each of the *M* sites has been tested to transfer charge to or from the electrode. Typically, the equilibrium state can be well reproduced after discarding the first 5×10^6 MCSs. Then, the next 2×10^6 MCSs are used to compute averages. 500 different initially random configurations were used.

3. Results and discussions

The electrode surface is represented as a square lattice of L=256, and there are no sizes effects observed. For simplicity, the chemical potential and the lateral energies are expressed in k_BT units. Periodic boundary conditions are considered. The electrosorption valence is set to value, $\gamma = 1$.

In first place, it is described the formation of the c(2x2) structure without species *B* (σ = 0). Figure 2 show, in the same axis, the order parameter, adsorption isotherm, and current, versus E/k_BT , for w/k_BT=4.0 as the energy value chosen to observe the ordered phase. The c(2x2) structure is fully formed at a half of the surface coverage, and it is seen as a broad plateau in the isotherm.

The order parameter reaches the value 1.0 at the same potential range of the isotherms plateau. When the coverage is less or more than the half coverage, the structure is imperfect, then Ψ tend to zero.

With respect to the voltammogram, the current shows two peaks before and after the formation of the c(2x2) structure. It is useful separate the analysis in three regions, delimited by dash line as is indicated in figure 2. Region I), at low potential values, before the first peak: The increase in fluctuations (current) is due to the availability of empty sites and the interaction energy between particles *A*. In the last case, the interactions cause the particles *A* to be deposited far from each other. The fluctuation and *i*, increases until a maximum, first positive current peak (i_{p-1}), that occurs before the formation of the half coverage (θ = 0.5) in the isotherm. This peak corresponds to the inflexion point before the formation of the plateau. Region II), between peaks: When the c(2x2) structure is formed, the fluctuations are strongly reduced, in correspondence with the broad plateau in the isotherm. As $\theta > 0.5$, the fluctuation and current rise until the formation of a second peak, i_{p-2}, which correspond to the second inflexion point in the isotherm. Finally the region III): after the second peak, where the

reduction of *i*, is due to the decrease of the empty sites and, when the surface is complete filled, at θ_s=1.0, the current drop to zero.

Now, the formation of the c(2x2) structure in presence of species *B* is analyzed. The order parameter Ψ versus E/k_BT for $0 \leq \sigma \leq 1$, is shown in figure 3(a). As σ increase Ψ is considerable reduced. This means that the order is reduced by the presence of particles *B* on the electrode surface, even at low σ values. To quantify this phenomenon it is possible to define a function as:

$$T(\sigma) \equiv \frac{\int \Psi(\sigma) dE}{\int \Psi(\sigma = 0) dE} \tag{5}$$

The parameter T(σ) is a quotient of areas between the clean surface, σ=0, and any other case. Their values are an indicator of the σ influence in the ordering of species *A* at the electrode. In figure 3(b) T(σ) versus σ is shown. It can be seen that the order decreases drastically from σ = 0.0 to σ = 0.1, then the decrease is slower until tend to zero. To understood how particles *B* affect the order, it is important to observe that even at low σ values the c(2x2) structure is destroyed Figure 4, shows a snapshot of the lattice status at σ=0.1. The blue dots are particles *B*, blacks are particles *A* and white are empty sites. The boundaries of regions with different degenerations, delimited by red lines in figure 4, can generally be identified by the following : Particles B which reduce the coordination of particles A adsorbed in their neighborhoods and nearest neighbors with the same occupation (indicated by rectangles in figure 4). Figure 5(a) show the adsorption isotherms (E/k_BT *versus* θ) for different σ values. As σ increase the plateau begins to be less wide until, at σ>0.4, is difficult to distinguish and for σ>0.6, disappear completely. All isotherms saturate at the value θ_s=1-σ respectively, as is expected. This is in complete agreement with analyzes performed for the order parameter.

Figure 5(b) shows the simulated voltammograms (E/k_BT *versus* i) at different σ values. Several observations can be made. For σ > 0.0, the first peak is more intense than the second, $i_{p-1} > i_{p-2}$ and i_{p-2} tend to disappear as σ grows up. This can be understood because the fluctuations (and hence the charge transfer) are more important in situations where there are more vacancy sites, specifically at low coverages. The analysis is separated in three region like has been done before. In region (I), as σ increases, the first peak decreases because the availability of empty sites is reduced, but the potential peak E_{p-1} does not show substantial shifts. In region (II), between the peaks, depositions of particles *B* reduce the order of the c(2x2) structure. Particles *B* favor the deposition on the structure because the energy associated to the deposition, in average, is smaller than when the structure is perfectly formed (σ=0). This phenomenon causes that i increase. But this effect is reduced as σ>0.6, because the empty sites are reduced, and the c(2x2) is not observed in the substrate. Finally, in region (III), after i_{p-2}, when the order is destroyed in all cases, the plateaus of the isotherms are less visible. The second inflexion point is displaced toward low potentials, as well as the position of the i_{p-2}. But, when σ>0.6, the second peak and the ordered phase disappears completely, as expected.

If we compare Figures 5 (a) and (b) in a single view, and with the support of previous analyzes, it is easy to understand that voltammograms provide more detailed information than isotherms to describe physical processes occurring on the surface. Especially in cases like in the present work, where plateaus and inflection points undergo modifications as the electrode surface is altered.

Now, we are interested in analyze the effect of the interactions at σ constant. Figure 6 (a-c) shows adsorption isotherms, order parameter and current, for σ=0.1, at w/k_BT=0.0, 0.5, 1.0, 2.0 and 4.0. At w/k_BT=0.0, the isotherm have a sigmoidal shape and saturate at θ_s=0.9, as expected. The order parameter is less than 5%, this means there is no order on the lattice. The

current show only one peak, intense, at E/k_BT=0.0; because, in the absence of interactions, the only limitation of charge transfer is the availability of empty sites. When w/k_BT>0.0 the isotherms show a broad plateau and the order parameter is higher as the interactions becomes more intense. Moreover, the current peak decrease because, as the interaction is strongly, fluctuations decrease, but the potential peak it is not affected, and when w/k_BT>1.0 the second peak begins to be observed. Then the separation of peaks increases as the interaction increases.

The figure 7 shows the configurational entropy S, defined by equation (7), for the two cases previously analyzed. In the inset a), S versus θ for several σ values at w/k_BT=4, is shown. At a clean surface (σ=0.0), three minimums are observed in correspondence with the three ordered states; empty surface (θ=0.0), c(2x2) structure (θ=0.5) and at full coverage (θ_s=1.0). All the central minimums match with the coverage where the plateaus are formed and with θ_s, as expected. Between these minimums, two maximums are observed (θ=1/4, 3/4); these correspond to the disordered states. As σ increase both maximums decrease, and the minimum associated with c(2x2) structure increase, this is evidence that particles *B* weaken order. But, for σ≥0.4, the second maximum disappears like the plateaus in the isotherms.

The inset b) shows the entropy for σ=0.1 and several values of w/k_BT. For the case without interactions, Langmuir case w/k_BT=0.0, the lobule is completely symmetric respect θ≈0.45. As w/k_BT increase, the lobule decreases until a minim appears in correspondence with the formation of the order structure and the plateau in the isotherm. These minima are deeper around θ≈0.45 and are more asymmetric upon w/k_BT increase. As the particles *B* affect more the order to high coverage, the second maximum is less intense that the first. The configurational entropy is in concordance with the isotherms analysis.

In other hand, it is possible to use the minimums of the configurational entropy to infer how σ affects the critical temperature $T_C(L)$, of the c(2x2) phase transition. The entropy versus

k_BT at the constant σ, presents an inflection point at k_BT_C. This behavior is shown in Figure 8, for σ = 0.1. To obtain this value, is easy consider the maximum of the derivative of S respect to k_BT, as shown in the inset (a) of Fig.8 . In inset (b) $k_BT_C(L)$ (in units of, k_BT_C(L=256, σ=0) =2.24(2)) versus σ is shown. By means of a linear fit, one gets k_BT_C (σ) = 0.99(2)-1.29(2)σ. As expected, T_C decrease with increasing particles *B* amount.

Finally, it is analyzed the behavior of voltammograms at high values of w/k_BT and several values of σ. Figure 9(a) shows a voltammogram for w/k_BT=6.0 and σ=0.0, 0.1, 0.2, 0.3 and 0.5.

In this case, in addition to the "two peaks" analysis already described, two and three new small peaks are observed for σ> 0.0, those peaks are marked with a blue arrow. These peaks appear due to the strong repulsion between species *A*, and can be used to describe different sites environments, as E/k_BT increase. In Figure 9(b), the peaks are labeled from (i) to (v) for w/k_BT=6.0 and σ= 0.5. Before the peak (i), the less energetic environment is surrounded by empty sites, particles *B*, or a combination of both. The filling of this environment, at low potentials, is the main responsible of the mayor peak. In the Figure 9 (b), the "snapshot" shows an example of this environment of empty sites (white dots): red dots are empty sites or particles *B* and blue dots are particles *A.* The blue arrows indicate that the central empty site will be occupied after the peak. Then, at the peak (ii), the less energetic environment is those with just one particle *A*. The other peaks (iii-v) can be understood in the same way, where the environments that need more energy to occupy the central site, are those surrounded by a greater number of particles *A*. Hence, in this situation, particles *B*, favor the transient states.

4. Conclusions

In this work, standard Monte Carlo simulation in the Gran Canonical Ensemble was used in order to study the electrosorption on a modified electrode surface. The main objective

was to analyze how the depositions of non-electroactive particles on the electrode surface, affect the criticality of phase c (2x2).

A square lattice-gas model was used to define the electrode surface. Two species were adsorbed: specie *A*, electroactive, and *B*, non-electroactive. The density of each one was called θ and σ, respectively. Only repulsive interactions, in k_BT units (w/k_BT), between particles *A* were considered.

Several conclusions can be drawn:

1. At low density of σ, the c(2x2) structure is destroyed, because the species *B* delimit regions, like domain boundaries. These limits prevent the order of the structure c (2x2) from reaching the entire system.
2. As σ increase, the plateau in the isotherms begins to be less wide, until at σ>0.6, disappears completely. The particles *B* weaken the c(2x2) structure, the plateaus increases in its slope.
3. The voltammograms shows two peaks for different σ values: The first peak is more intense than the second because the fluctuations are more important at low coverages. As σ increases, the first peak decreases because empty sites decrease. Particles *B* favor the deposition of particles *A* on the c(2x2) structure, this causes the current increase, at the cost of destroying the phase order. At σ>0.6, the second peak disappears.
4. The configurational entropy per site, shows two lobules, separate by three minimums in correspondence with empty lattice, c(2x2) structure (θ=0.5) and full occupied lattice (θ=1.0). As σ increase the lobules and the minimum associated to c(2x2) structure decreases. This in complete agreement with the previous analysis realized to isotherms and voltammograms.
5. With the configurational entropy, it was possible to obtain a decreasing linear relationship between T_C and σ.

6. At high interaction energy, several contributions of transient estates were manifested as current peaks in the voltammograms, each peak correspond to the filling of different environments, around an empty central site.

6. Acknowledgements

This work was supported in part by CONICET (Argentina) under project number PIO 112-201101-00615. Universidad Nacional de Santiago del Estero (Argentina), under project CICyT-UNSE 23 A 212.

The simulations were carried out on a HUAUKE parallel cluster located at Instituto de Bionanotecnología del NOA, Universidad Nacional de Santiago del Estero, Santiago del Estero, Argentina.

References

[1] T. Nann and J. Heinze, "Simulation in electrochemistry using the finite element method: Part 1: The algorithm," *Electrochem. commun.*, vol. 1, no. 7, pp. 289–294, 1999.

[2] R. G. Compton, E. Laborda, and K. R. Ward, *Understanding Voltammetry: Simulation of Electrode Processes*. Singapore, 2013.

[3] D. Britz, *Digital Simulation in Electrochemistry*, Third. Berlin, Heidelberg, 2005.

[4] K. Binder;, "Simulation of Diffusion in Lattice Gases and Related Kinetic Phenomena, Applications of the Monte Carlo Method in Statistical Physics, Topics in Current Physics V," vol. 36, K. Binder, Ed. Berlin: Springer, 1987, p. 181.

[5] A. J. Bard, J. A. Crayston, G. P. Kittlesen, T. Varco, and M. S. Wrighton, "Digital Simulation of the Measured Electrochemical Response of Reversible Redox Couples at

Microelectrode Arrays : Consequences Arising from Closely Spaced Ultramicroelectrodes," pp. 2321–2331, 1986.

[6] H. Yang and A. J. Bard, "The application of rapid scan cyclic voltammetry and digital simulation to the study of the mechanism of diphenylamine oxidation , radical cation dimerization , and polymerization in acetonitrile," vol. 306, pp. 87–109, 1991.

[7] K. Binder, *Monte Carlo Methods in Statistical Physics (Topics in Current Physics)*, vol. 7. Berlin: Springer, 1978.

[8] K. Binder, "Applications of Monte Carlo methods to statistical physics," vol. 60, pp. 487–559, 1997.

[9] K. Binder and D. Heermann, *Monte Carlo Simulation in Statistical Physics - An Introduction*, 5th ed. Berlin: Springer, 2010.

[10] D. Nicholson and N. G. Parsonage, *Computer Simulation and the Statistical Mechanics of Adsorption*. London, New York: Academic Press, 1982.

[11] A. Patrykiejew, S. Sokoøowski, K. Binder, È. Physik, and È. Mainz, "Phase transitions in adsorbed layers formed on crystals of square and rectangular surface lattice," *Surf. Sci. Rep.*, vol. 37, pp. 207–344, 2000.

[12] G. Brown, P. A. Rikvold, S. J. Mitchell, and M. a. Novotny, "Monte Carlo Methods for Equilibrium and Nonequilibrium Problems in Interfacial Electrochemistry," *Computer (Long. Beach. Calif).*, p. 14, 1998.

[13] P. A. Rikvold, I. A. Hamad, T. Juwono, D. T. Robb, and M. A. Novotny, "Modern Aspects of Electrochemistry No. 44," no. 44, New York: Springer, 2009, pp. 131–149.

[14] S. J. M. P.A Rikvold, G. Brown, "Statistical mechanics of lattice models of electrochemical interfaces, in: A. Hubbard (Ed.) Encyclopedia of Surface and Colloid Science, Dekker," New York (2002), 2002, p. 4814.

[15] M. T. M. Koper, "A lattice-gas model for halide adsorption on single-crystal

electrodes," *J. Electroanal. Chem.*, vol. 450, no. 2, pp. 189–201, 1998.

[16] M. T. . Koper, "Monte Carlo simulations of ionic adsorption isotherms at single-crystal electrodes," *Electrochim. Acta*, vol. 44, no. 6–7, pp. 1207–1212, 1998.

[17] T. Wandlowski, J. X. Wang, and B. M. Ocko, "Adsorption of bromide at the Ag (100) electrode surface," *J. Electroanal. Chem.*, vol. 500, no. 1, pp. 418–434, 2001.

[18] S. J. Mitchell, G. Brown, and P. A. Rikvold, "Static and dynamic Monte Carlo simulations of Br electrodeposition on Ag(1 0 0)," *Surf. Sci.*, vol. 471, no. 1–3, pp. 125–142, 2001.

[19] H. Bort, K. Jüttner, W. J. Lorenz, G. Staikov, and E. Budevski, "Underpotential-overpotential transition phenomena in metal deposition processes," *Electrochim. Acta*, vol. 28, no. 7, pp. 985–991, 1983.

[20] B. Ocko, J. Wang, and T. Wandlowski, "Bromide Adsorption on Ag(001): A Potential Induced Two-Dimensional Ising Order-Disorder Transition," *Phys. Rev. Lett.*, vol. 79, no. 8, pp. 1511–1514, 1997.

[21] H. Siegenthaller, K. Juttner, E. Schmidt, and W. J. Lorenz, "Voltammetric Investigation Of Thallium Adsorption on Silver Single Crystal Electrodes," *Electrochim. Acta*, vol. 23, pp. 1009–1018, 1978.

[22] H. Bort, K. Jüttner, W. J. Lorenz, and E. Schmidt, "Lead adsorption on silver single crystal surfaces," *J. Electroanal. Chem.*, vol. 90, no. 3, pp. 413–424, 1978.

[23] W. Rudzinski and D. H. Everett, *Adsorption of Gases on Heterogeneous Surfaces*. Elsevier, 1991.

[24] M. J. Jaroniec and R. Madey, *Physical Adsorption on Heterogeneous Surfaces*. Amsterdam: Elsevier, 1988.

[25] W. Rudzinski, W. A. Steele, and G. Zgrablich, *Equilibria and Dynamics of Gas Adsorption on Heterogeneous Solid Surfaces*. Amsterdam: Elsevier, 1996.

[26] M. Quintana, M. Pasinetti, A. J. Ramirez-pastor, and G. Zgrablich, "Adsorption thermodynamics of monomers on diluted-bonds triangular lattices," vol. 600, pp. 33–42, 2006.

[27] M. a Perarnau, P. M. Centres, F. Bulnes, and a J. Ramirez-Pastor, "Critical behavior of repulsively interacting particles adsorbed on disordered triangular lattices.," *Phys. Chem. Chem. Phys.*, vol. 12, no. 40, pp. 13280–6, 2010.

[28] A. N. Kuznetsov, V. I. Zaikovskii, V. N. Parmon, and E. R. Savinova, "Site Blocking with Gold Adatoms as an Approach to Study Structural Effects in Electrocatalysis," pp. 211–220, 2012.

[29] A. Zolfaghari, F. Villiard, M. Chayer, and G. Jerkiewicz, "Hydrogen adsorption on Pt and Rh electrodes and blocking of adsorption sites by chemisorbed sulfur," *J. Alloys Compd.*, vol. 253, pp. 481–487, 1997.

[30] F. Hernandez and H. Baltruschat, "Hydrogen evolution and Cu UPD at stepped gold single crystals modified with Pd," *J. solid state Electrochem.*, vol. 11, pp. 877–885, 2007.

[31] R. R. Adžić and J. X. Wang, "Configuration and Site of O_2 Adsorption on the Pt(111) Electrode Surface," *J. Phys. Chem. B*, vol. 102, no. 45, pp. 8988–8993, 1998.

[32] E. Leiva, T. Iwasita, E. Herrero, and J. M. Feliu, "Effect of Adatoms in the Electrocatalysis of HCOOH Oxidation. A Theoretical Model," *Langmuir*, vol. 13, no. 23, pp. 6287–6293, 1997.

[33] L. Guohua, H. Ikuta, T. Uchida, and M. Wakihara, "The Spinel Phases LiMMn2.,O4 (M = Co, Cr, Ni) as the Cathode for Rechargeable Lithium Batteries," vol. 143, no. 1, pp. 178–182, 1996.

[34] M. P. Mercer, S. Finnigan, D. Kramer, D. Richards, and H. E. Hoster, "The influence of point defects on the entropy profiles of Lithium Ion Battery cathodes: a lattice-gas

Monte Carlo study," *Electrochim. Acta*, vol. 241, pp. 141–152, 2017.

[35] A. J. Bard and L. R. Faulkner, *Electrochemical Methods : Fundamentals and Applications*. 2001.

[36] W. Schmickler and E. Santos, *Interfacial Electrochemistry*, Second. 2010.

[37] E. Gavilán Arriazu, V. I. P. Zanini, F. A. Gulotta, and V. M. Araujo, "Electrochemical behavior of a typical redox mediator on a modi fi ed electrode surface : Experiment and computer simulations," *Surf. Sci.*, vol. 658, no. July 2016, pp. 15–21, 2017.

[38] J. W. Schultze and K. J. Vetter, "In contrast to adsorption from the gas phase , electrosorption depends on the," *Electroanal. Chem. Interfacial Electrochem.*, vol. 44, pp. 63–81, 1973.

[39] I. A. Hamad, S. J. Mitchell, T. Wandlowski, P. A. Rikvold, and G. Brown, "Cl electrosorption on Ag(1 0 0): Lateral interactions and electrosorption valency from comparison of Monte Carlo simulations with chronocoulometry experiments," *Electrochim. Acta*, vol. 50, no. 28, pp. 5518–5525, 2005.

[40] I. Abou Hamad, T. Wandlowski, G. Brown, and P. A. Rikvold, "Electrosorption of Br and Cl on Ag(1 0 0): Experiments and computer simulations," *J. Electroanal. Chem.*, vol. 554–555, no. 1, pp. 211–219, 2003.

[41] I. A. Hamad, P. A. Rikvold, and G. Brown, "Determination of the basic timescale in kinetic Monte Carlo simulations by comparison with cyclic-voltammetry experiments," *Surf. Sci.*, vol. 572, no. 2–3, pp. 1–14, 2004.

[42] O. A. Pinto, B. A. López de Mishima, E. P. M. Leiva, and O. A. Oviedo, "Monomolecular adsorption on nanoparticles with repulsive interactions: a Monte Carlo study," *Phys. Chem. Chem. Phys.*, vol. 18, no. 21, pp. 14610–14618, 2016.

[43] G. T. B. M.E.J. Newman, *Monte Carlo Method in statistical physics*. Clarenton –Press Oxford, 1999.

[44] H. B. Callen, *Thermodynamics and an Introduction to Thermostatistics*. John Wiley and Sons, 1985.

[45] M. T. M. Koper, A. P. J. Jansen, and R. A. Van Santen, "Monte Carlo simulations of a simple model for the electrocatalytic CO oxidation on platinum," vol. 109, no. 14, 1998.

[46] C. Saravanan, M. T. M. Koper, N. M. Markovic, M. Head-Gordon, and P. N. Ross, "Modeling base voltammetry and CO electrooxidation at the Pt(111)-electrolyte interface: Monte Carlo simulations including anion adsorption," *Phys. Chem. Chem. Phys.*, vol. 4, no. 111, pp. 2660–2666, 2002.

[47] O. A. Pinto, A. J. Ramirez-Pastor, and F. Nieto, "Phase diagrams for the adsorption of monomers with non-additive interactions," *Surf. Sci.*, vol. 651, pp. 62–69, 2016.

[48] K. B. D. Stauffer;, "Applications of the Monte Carlo, Method in Statistical Physics," Vol. 36,., vol. 36, K. Binder, Ed. Springer, Berlin, 1984., 1984, p. 1984.

[49] N. Metropolis, A. W. Rosenbluth, M. N. Rosenbluth, A. H. Teller, and E. Teller, "Equation of state calculations by fast computing machines," *J. Chem. Phys.*, vol. 21, no. 6, pp. 1087–1092, 1953.

Figure captions

Figure 1 : Scheme of the lattice in which two sub-lattices, 1 and 2, are identified.

Figure 2: The surface coverage, order parameter and current, versus E/k_BT , for w/k_BT=4.0. Dash line separate regions I, II and III.

Figure 3: a) The order parameter Ψ versus E/k_BT for $0 \leq \sigma \leq 1$ b) T(σ) versus σ

Figure 4: Snapshot of the lattice status at σ=0.1. The blue dots are particles *B*, blacks are particles *A* and white are empty sites. Blue ellipses were included for the identification of at the boundaries of regions with different degenerations. Red lines delimit regions with different degenerations

Figure 5: Fort different σ values: a) Adsorption isotherms, E/k_BT versus θ, b) Simulated voltammograms, E/k_BT versus i .

Figure 6 : For σ=0.1, and several values of w/k_BT. a) adsorption isotherms, b)order parameter and c) current.

Figure 7: a) Configurational entropy S, versus θ. for several σ values. b) Configurational entropy for σ=0.1 and several values of w/k_BT.

Figure 8: S versus k_BT, at σ=0.1. a) Derivative of S respect to k_BT. b) $k_BT_C(L)$ / k_BT_C(L=256, σ=0) versus σ.

Figure 9: a) Voltammograms for w/k_BT=6.0 and several σ values. b) Voltammogram for w/k_BT=6.0 and σ=0.5. Peaks are labeled from (i) to (v). Snapshots: environment of an empty site, red dot are empty sites or particles B and blue dots are particles A.

Figure 1

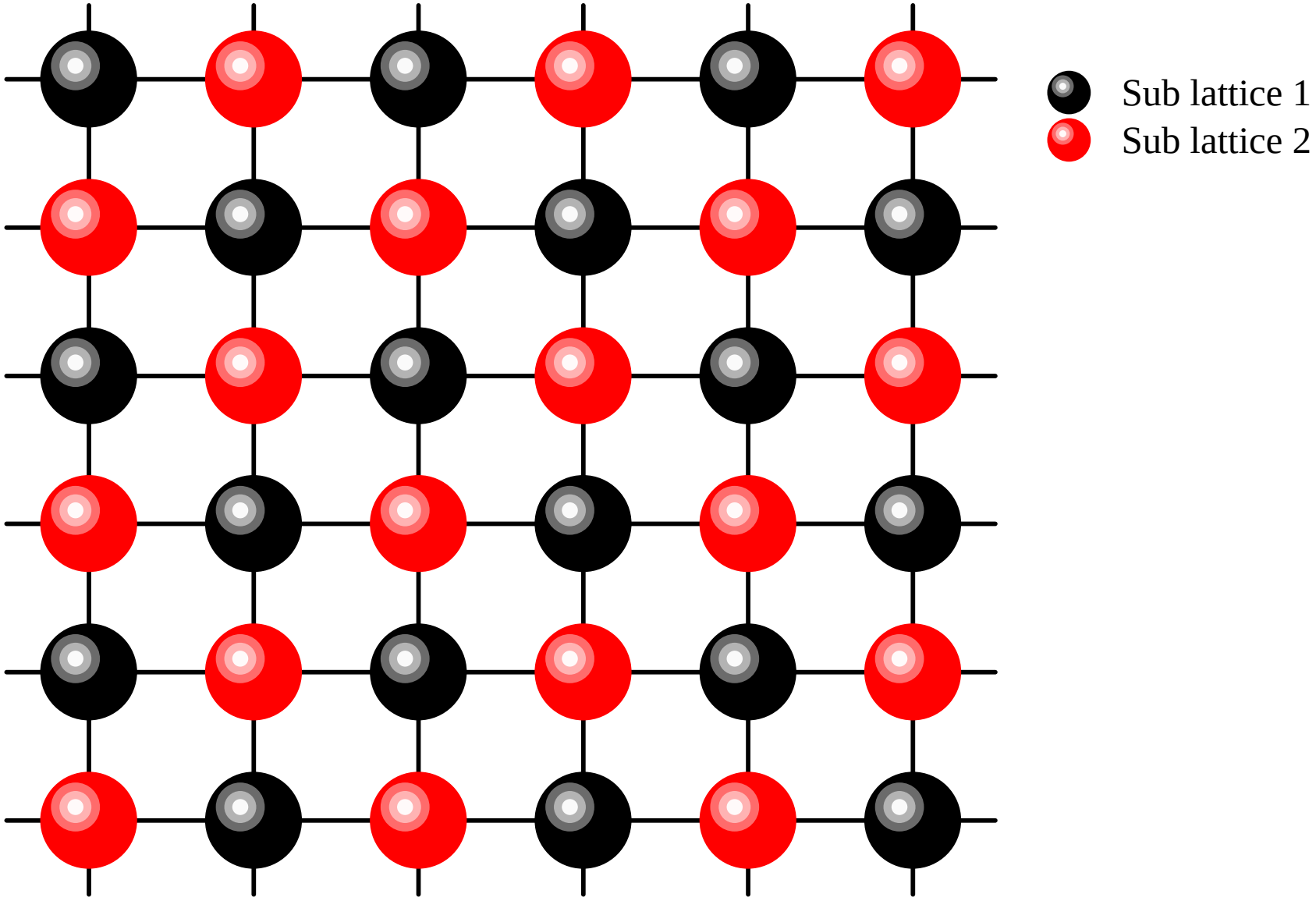

Figure 2

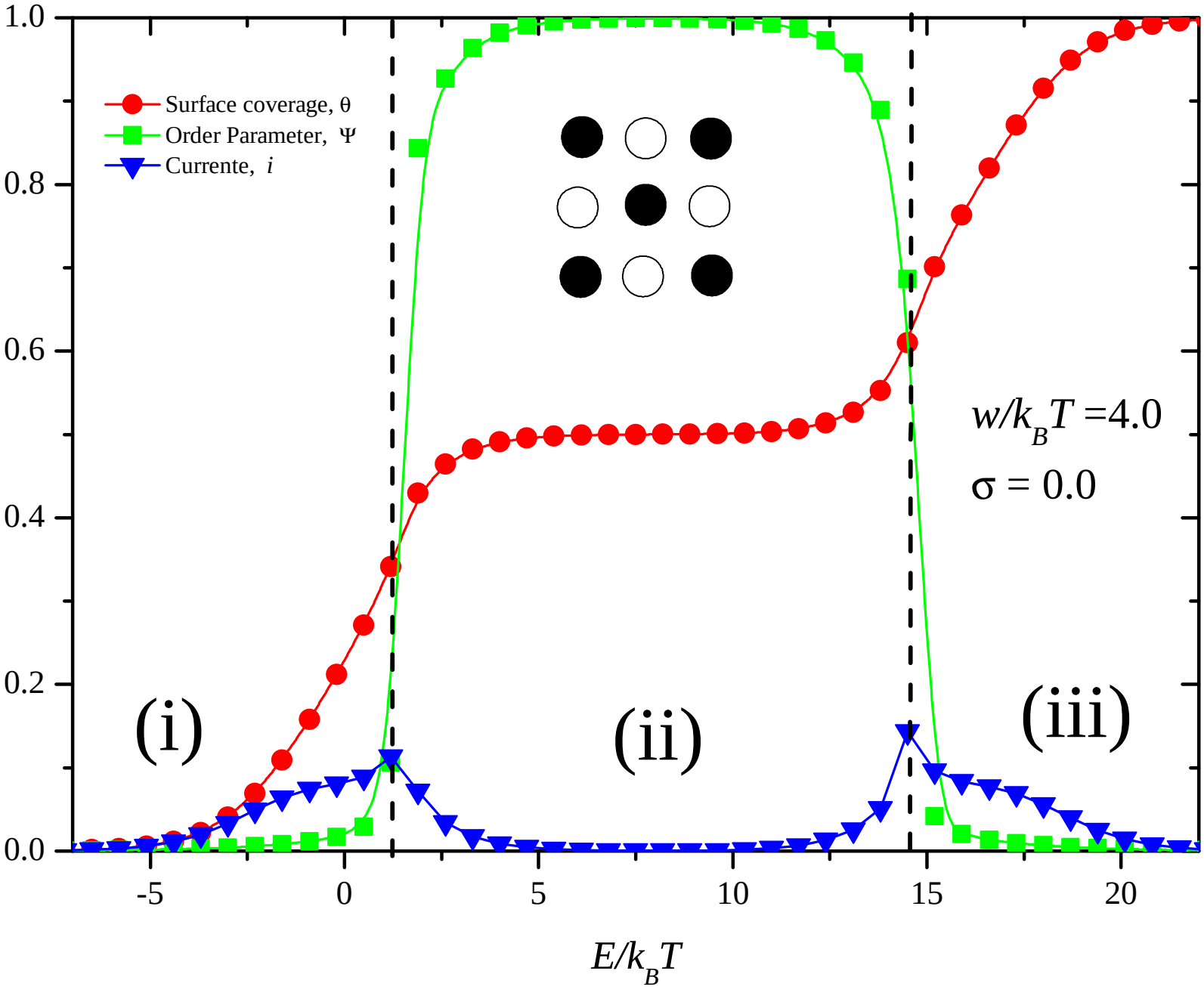

Figure 3

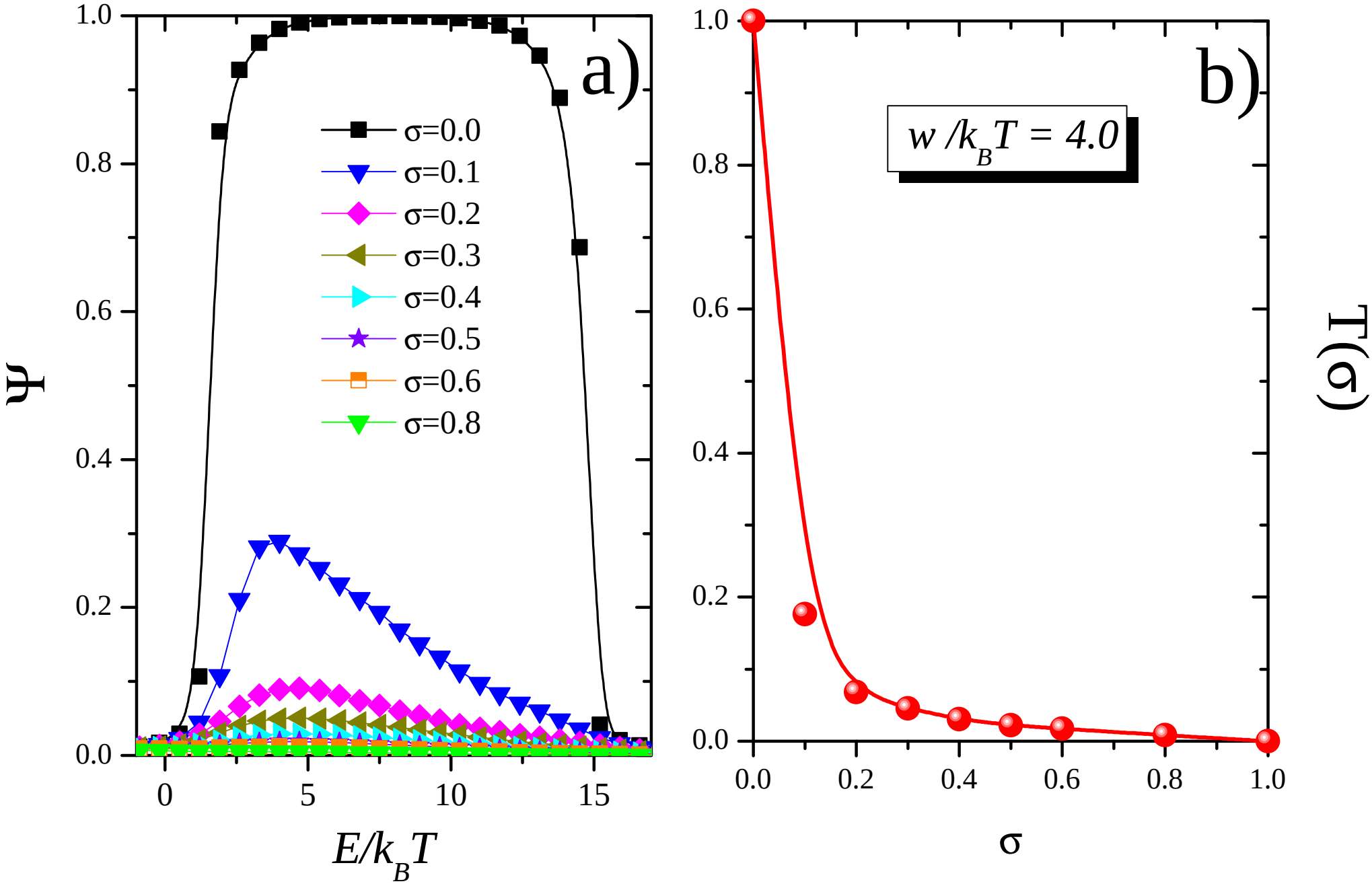

Figure 4

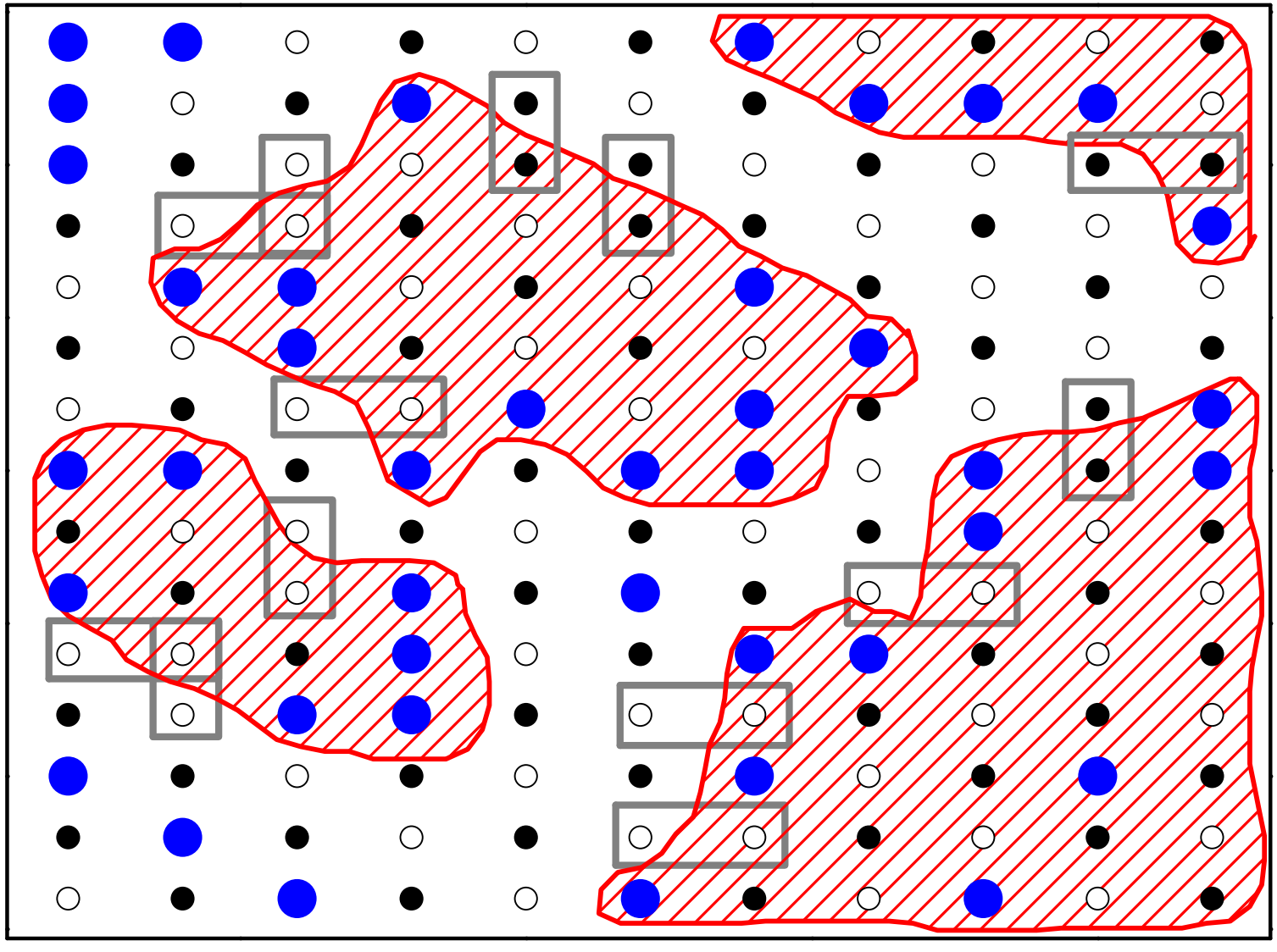

Figure 5

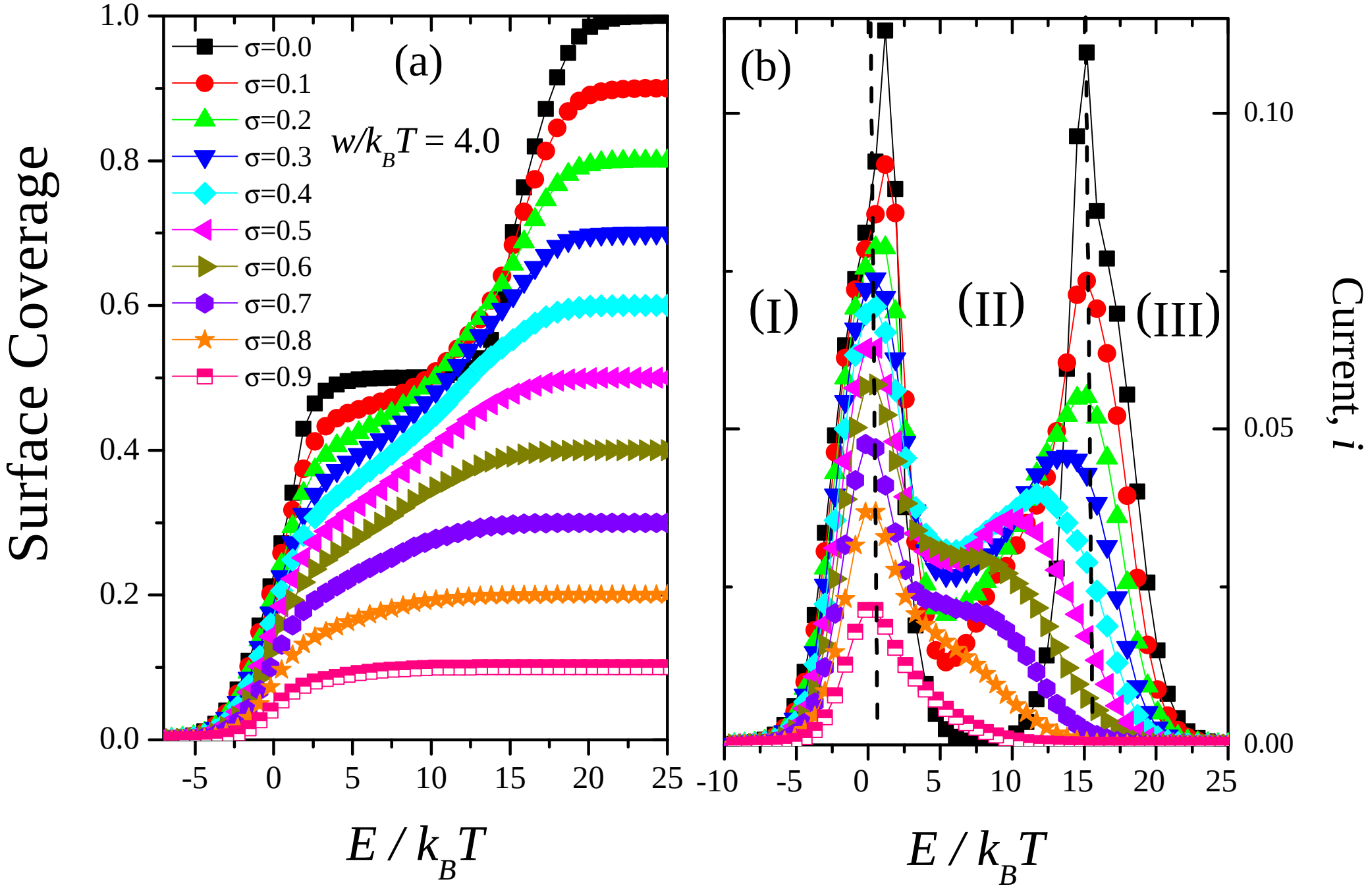

Figure 6

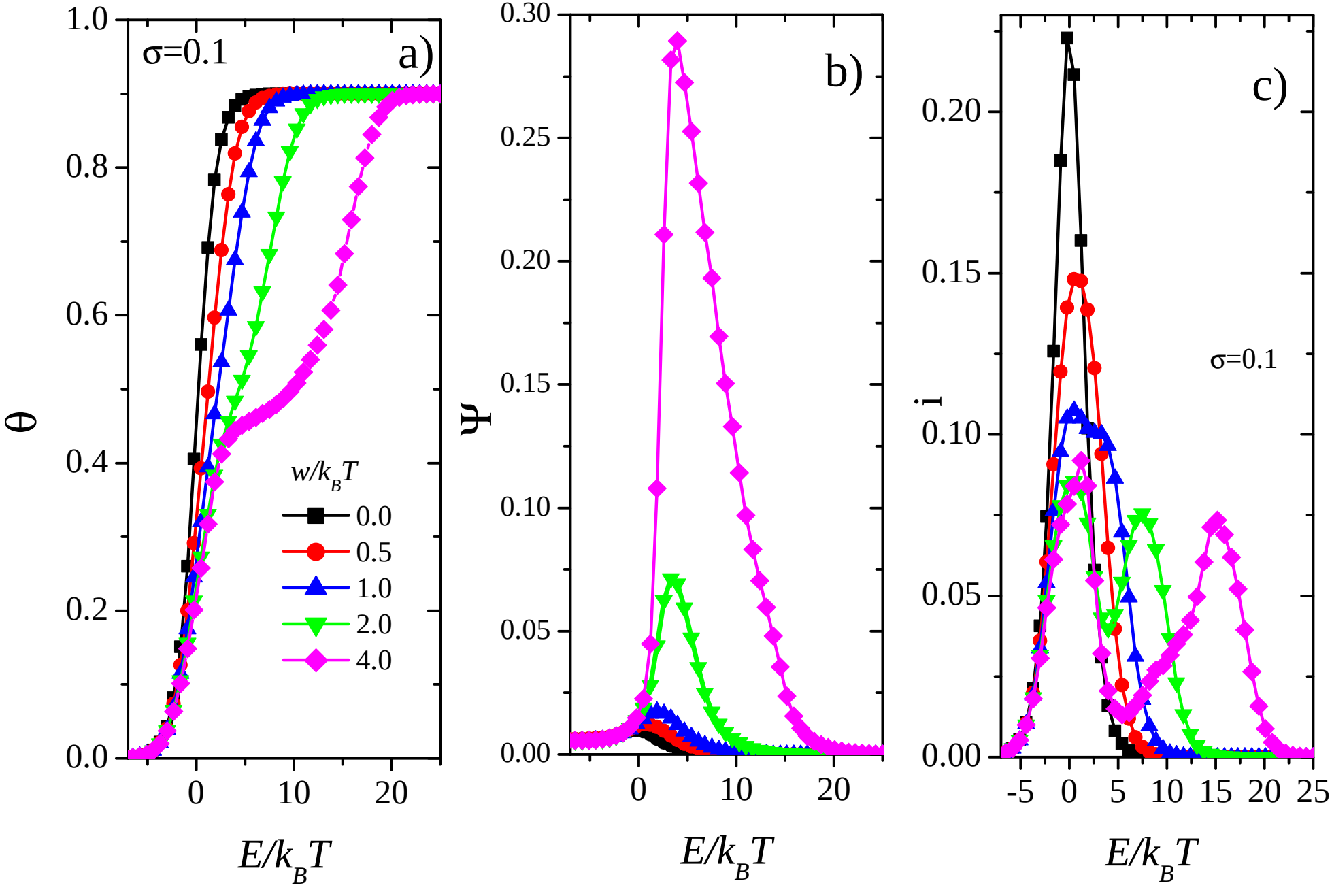

Figure 7

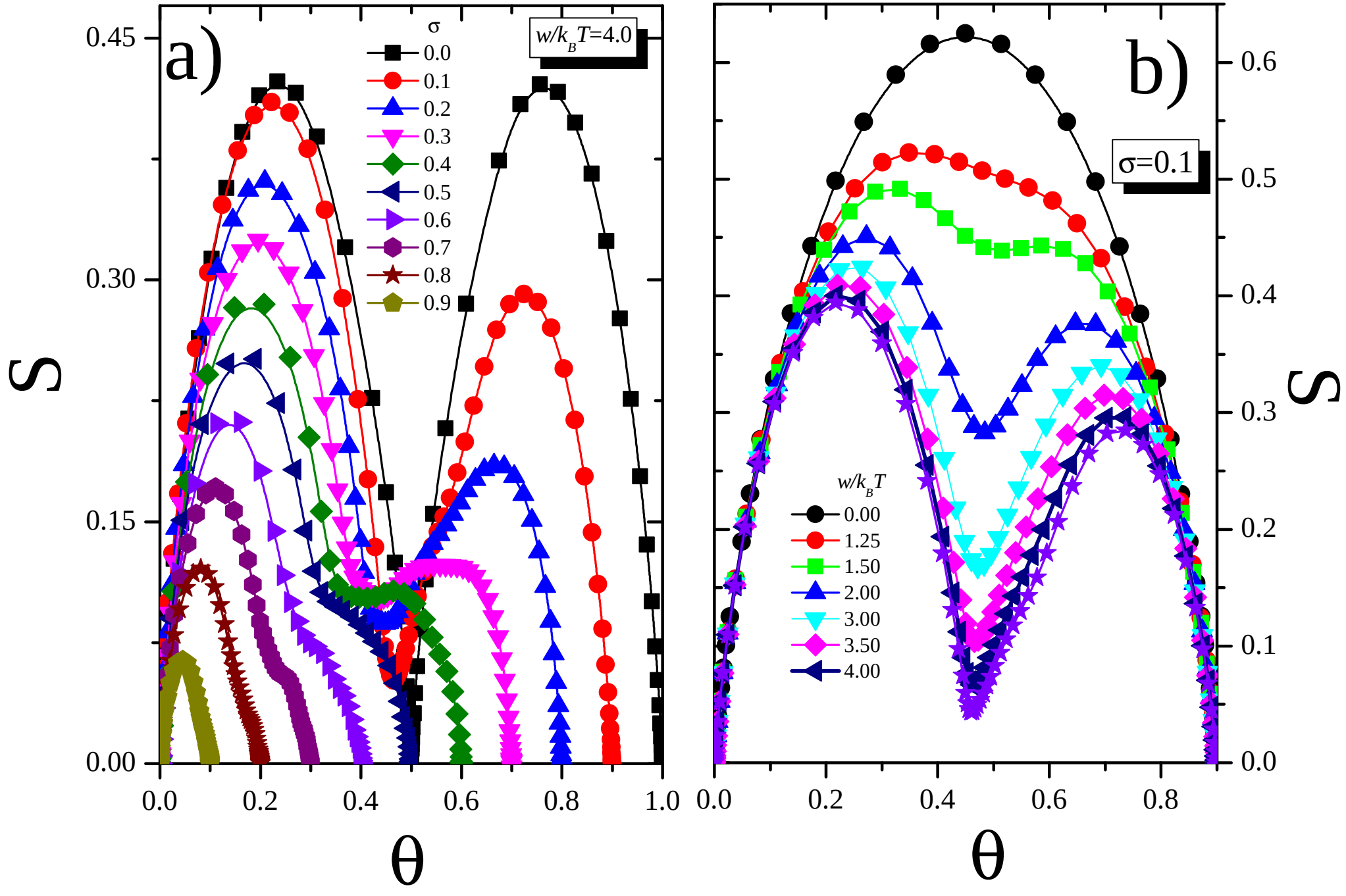

Figure 8

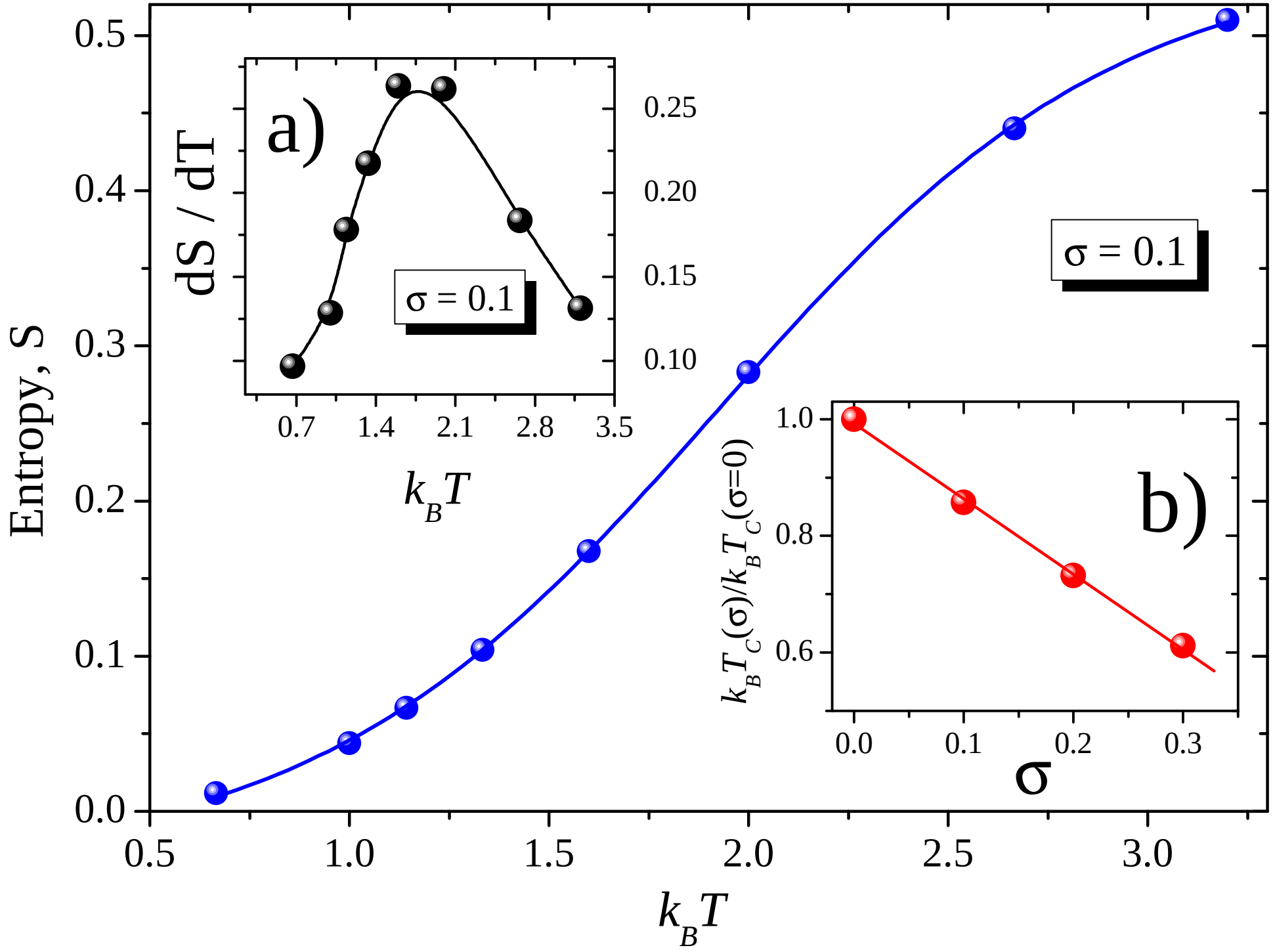

Figure 9